*Inst. Phys. Conf. Ser. No 175*
*Paper presented at 7th Int. Conf. Computational Accelerator Physics, Michigan, USA, 15–18 October 2002*



# Muon beam ring cooler simulations using COSY INFINITY

**Carlos O. Maidana†, Martin Berz† and Kyoko Makino‡**

† Department of Physics and Astronomy, Michigan State University, East Lansing, MI 48824, USA
‡ Department of Physics, University of Illinois at Urbana-Champaign, 1110 W. Green Street, Urbana, IL 61801-3080, USA

E-mail: maidanac@msu.edu, berz@msu.edu, makino@uiuc.edu

**Abstract.** In this paper we present simulations using COSY INFINITY to study the behavior of muon beams in a ring cooler designed by V. Balbekov[1]. Because of the substantial transversal emittance, the nonlinearities play a very important limiting role that must be understood and controlled well, which leads to the requirement of high order computation. We describe the system, the approaches for the simulations of the large aperture solenoids and magnetic sectors, and we show the nonlinear transfer maps as well as tracking simulations for different field models, and compare with other methods based on various approximations.

PACS numbers: 02.60.Cb, 05.45.-a, 29.27.-a, 29.27.Eg, 41.85.-p, 41.85.Ja, 41.85.Lc

## 1. The ring and the simulation approaches

Various designs and ideas have been developed for cooling of short lived muon beams in neutrino factories and muon colliders[2]. The concept of cooling is based on ionization through material[3, 4, 5, 6], and to reduce cooling time, normally the system has a combined structure, consisting of absorbing material, accelerating cavities and guiding magnets[2, 7]. Because of the huge transversal emittance of muon beams, the consideration of nonlinear effects is an essential component in an earlier design stage. Lately, several designs of ring coolers have been considered because of the ability to utilize cooling sections repeatedly, and the additional potential for transversal and longitudinal emittance exchange. In this paper, we analyze a muon beam ring cooler designed by V. Balbekov[1]. The layout of the system is shown in Figure 1.

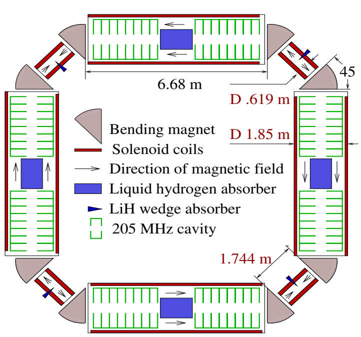


**Figure 1.** The layout of the tetra muon cooler designed by V. Balbekov[1].

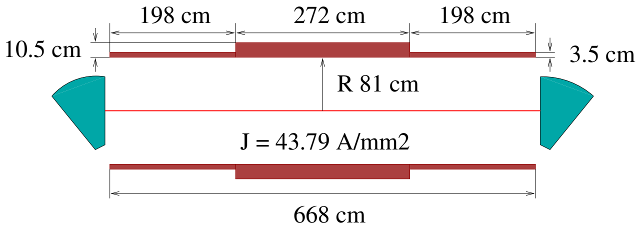


**Figure 2.** The parameters of the long straight solenoidal section[1].

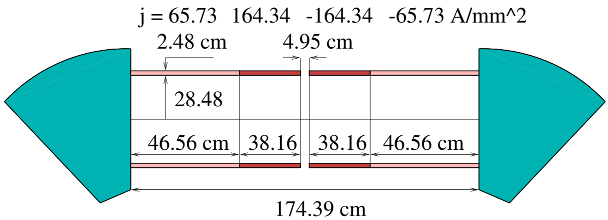


**Figure 3.** The parameters of the short straight solenoidal section[1].

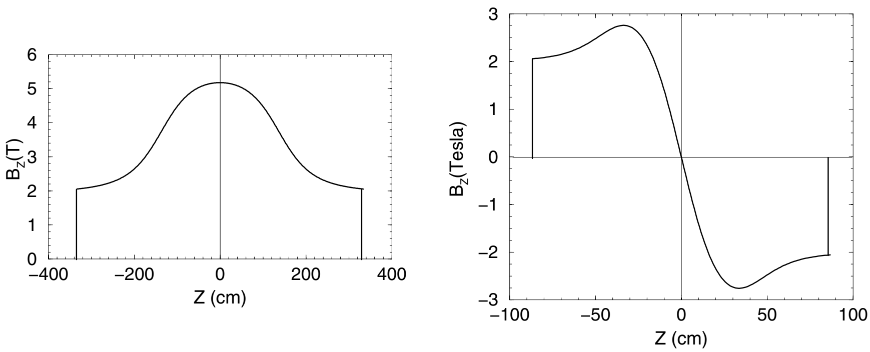


**Figure 4.** The hard edge model of the axial magnetic field in the long straight solenoidal section (left) and in the short straight solenoidal section (right), assuming the solenoid coils extend to infinity[1].

The ring consists of eight straight sections dominated by solenoids and eight inhomogeneous bending magnets[1]. The four long straight sections have absorbing material and accelerating cavities inside the solenoids, thus the aperture is very large. The parameters of the solenoids in the long section are shown in Figure 2. The four short straight sections have wedge absorbers to allow for transversal and longitudinal emittance exchange in the middle, where the longitudinal magnetic field component flips direction. The parameters of the solenoids in the short section are shown in Figure 3. Balbekov uses a hard edge model for all magnets, and for simplicity of design purposes, it is usually adequate to assume that the coil of the magnets extend to infinity[1]. The profiles of the longitudinal component of the axial fields are shown in Figure 4.

First, if the length of the solenoids is finite, the field profiles differ significantly. Second, in the long section, due to the huge aperture, the fringe field extension is exceedingly long[8]. Third, the hard edge model is somewhat unrealistic even for the case of ferromagnetic yokes designed to block the fall-off of the fields[1] because they apparently need to have an aperture large enough for passage of the muon beams that have large transversal emittance. Considering these, we study the effects due to the different treatment of the fields using the code COSY INFINITY[9]. The perhaps most realistic field treatment in the design stage is to assume finitely long solenoids as indicated in Figures 2 and 3 without assuming the presence of ferromagnetic yokes. Such field profiles are shown in Figures 5 and 6, including the outside fringe regions. The code COSY INFINITY allows the nonlinear treatment of such solenoidal fields including outside fringe field effects[9, 8]. For the purpose of comparison, we also study the hard edge model of the fields. Balbekov uses the following linear kicks applied to the transversal components of momentum to recover the most important edge field effect, namely the induced overall rotation of the particles:[10]

$$\Delta p_x = \frac{C}{2} B_z y, \quad \Delta p_y = -\frac{C}{2} B_z x, \tag{1}$$

where $\vec{p}$ is in MeV/c, $x$ and $y$ are in meter, $B_z$ is the longitudinal component of the axial field at the edge in Tesla, and $C = 299.79245$. We also use the same linear kicks when the hard edge model is used.

## 2. Transfer maps of solenoidal sections

We compare the effects of the different treatment of the solenoidal fields in the long and short straight sections. A long section consists of three solenoidal parts, and a short section consists of four solenoidal parts, with the longitudinal field flipping direction in the middle. Both the long and the short sections are designed to have stronger current toward the middle. Due to the flip of the field direction and the relatively small aperture, the short section is more readily treatable by various approximations.

### *2.1. Short straight section*

We compute the nonlinear transfer maps of the short section for different field models with the beam kinetic energy of 250 MeV. We list the transfer maps of the hard edge model of infinitely long solenoids first. For the purpose of comparison, we show the map without and with the linear kicks (1). Below, parts of the nonlinear transfer maps are shown in the notation of COSY INFINITY[9]. We observe that the linear $x$, $a(= p_x/p_0)$ terms and the linear $y$, $b(= p_y/p_0)$ terms are almost decoupled when the kicks are applied, while they are coupled without the presence of kicks. Thus, the linear kick approximation recovers the main point of the linear motion and one of its important physical properties.

In the subsequent excerpts from transfer maps, the four columns represent final horizontal position $x$ (in meter), final horizontal slope $a$, final vertical position $y$ (in meter), and final vertical slope $b$, as a polynomial in the initial conditions. The exponents of the polynomial are listed in the last column; for example, “4100” corresponds to the initial horizontal position raised to the fourth power, and the initial horizontal slope raised to the first. The top lines of the map represent the linear motion, and corresponds to the well-known transfer matrix (although the latter is usually shown as the transpose of our format).

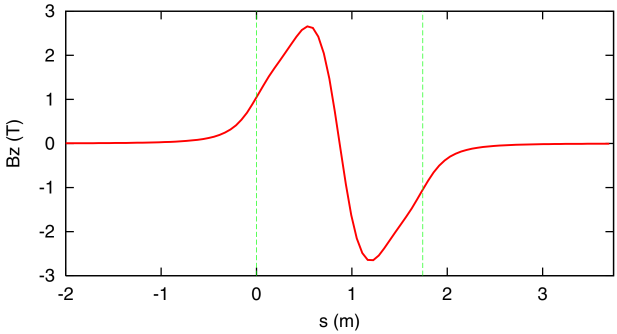


**Figure 5.** The axial magnetic field profile of the short section with finitely long solenoids and fringe fields.

**Hard edge model with infinitely long solenoids (no linear kicks)**

| x_f | a_f | y_f | b_f | xayb |
|---|---|---|---|---|
| -0.1467136 | -1.796260 | 0.9193886 | -0.2657072 | 1000 |
| 1.015304 | -0.1467136 | 0.3060451E-11 | 0.9193886 | 0100 |
| ... | ... | ... | ... | .... |
| -15.71585 | 27.23532 | -23.72338 | -33.63860 | 5000 |
| -36.02640 | 5.753202 | -21.46530 | -55.14127 | 4100 |
| -38.39075 | 16.29484 | -33.88081 | -55.16902 | 3200 |
| -33.14696 | -7.116152 | -14.53667 | -36.65477 | 2300 |
| -14.27604 | 2.840011 | -11.47237 | -15.47623 | 1400 |
| -7.567237 | -3.099152 | -1.462962 | -6.833978 | 0500 |

**Hard edge model with infinitely long solenoids with linear kicks**

| | | | | |
|---|---|---|---|---|
| -0.1467136 | -0.9637261 | -0.2022731E-03 | 0.5845774E-04 | 1000 |
| 1.015304 | -0.1467136 | 0.3060451E-11 | -0.2022730E-03 | 0100 |
| ... | ... | ... | ... | .... |
| -2.968705 | 1.388108 | 1.284507 | 1.099203 | 5000 |
| -12.74829 | -1.191336 | 1.970436 | 4.189763 | 4100 |
| -22.23560 | -5.817135 | -0.2996768 | 5.761626 | 3200 |
| -22.28744 | -10.62269 | -3.195642 | 4.297247 | 2300 |
| -15.60109 | -7.532831 | -4.618497 | 1.461128 | 1400 |
| -7.567237 | -4.424200 | -1.462962 | 0.1989097E-01 | 0500 |

We now list the same parts of the map of the hard edge model of finitely long solenoids. As seen in Figure 5, the edge field strength is about half of that with infinitely long solenoids. Thus, the map differs from the previous case, and the $(x,x)$ and $(a,a)$ terms show an obvious difference.

**Hard edge model with finitely long solenoids with linear kicks**

| | | | | |
|---|---|---|---|---|
| 0.3762572E-01 | -0.9144481 | 0.1324007E-03 | 0.9123892E-05 | 1000 |
| 1.092008 | 0.3762572E-01 | 0.1216993E-10 | 0.1324008E-03 | 0100 |
| ... | ... | ... | ... | .... |
| -4.559878 | 2.194351 | 1.925709 | 2.734348 | 5000 |
| -14.03917 | 1.790312 | 1.247951 | 8.100432 | 4100 |

| | | | | |
|---|---|---|---|---|
| -26.15120 | -0.5027561 | -4.741542 | 9.421870 | 3200 |
| -29.55137 | -6.150214 | -9.833677 | 4.913186 | 2300 |
| -20.98499 | -6.094498 | -8.584871 | -0.5031165 | 1400 |
| -8.419566 | -5.823382 | -1.776100 | -0.7673755 | 0500 |

We compare this map with the one computed for finitely long solenoids with correct outside fringe field consideration without using the linear kicks. These two maps agree well, confirming that the kick approach works well so far.

**Finitely long solenoids with correct fringe field consideration**

| | | | | |
|---|---|---|---|---|
| 0.9113584E-02 | -0.9101484 | 0.2707143E-04 | -0.8741688E-06 | 1000 |
| 1.098631 | 0.9113584E-02 | -0.1597370E-05 | 0.2707097E-04 | 0100 |
| ... | ... | ... | ... | .... |
| -4.919054 | 1.095873 | 0.6296333 | 1.603693 | 5000 |
| -14.58589 | 0.6387705 | -0.2037065 | 4.302134 | 4100 |
| -24.12332 | -1.227331 | -3.197581 | 3.442199 | 3200 |
| -26.81068 | -7.088700 | -4.268833 | -0.1562313 | 2300 |
| -19.59752 | -9.127604 | -2.390249 | -2.335453 | 1400 |
| -8.224955 | -7.060173 | 0.1989972 | -0.9178104 | 0500 |

### *2.2. Long straight section*

We performed the same study for the long straight section with the beam total energy of 250 MeV (the kinetic energy of 144.32 MeV). The hard edge model is used for infinitely long solenoidal field, and for finitely long solenoidal field, where the edge field strength is again about half of that with infinitely long solenoids. The computed transfer maps are compared to the one with the correct outside fringe field consideration. Since no good agreement was found between those three maps even in linear terms, we list only a part of the linear terms below.

**Hard edge model with infinitely long solenoids with linear kicks**

| | | | | |
|---|---|---|---|---|
| 0.7201144 | 0.6140963 | 0.4256817 | 0.3629942 | 1000 |
| -0.3623067 | 0.7201318 | -0.2141606 | 0.4256523 | 0100 |

**Hard edge model with finitely long solenoids with linear kicks**

| | | | | |
|---|---|---|---|---|
| -0.1764031E-02 | 0.4682935E-01 | -0.3214589E-01 | 0.9457639 | 1000 |
| -0.5217216E-01 | -0.1420209E-02 | -1.053667 | -0.3216291E-01 | 0100 |

**Finitely long solenoids with correct fringe field consideration**

| | | | | |
|---|---|---|---|---|
| 0.2334781 | 0.7546891 | 0.8859026E-01 | 0.2042114 | 1000 |
| -1.157656 | 0.2462930 | -0.3132503 | 0.4123110E-01 | 0100 |

The main reason for the disagreement between the hard edge model and the correct fringe field treatment is due to the limitation of the linear kick approximation in (1). Comparing the field profiles between the short section in Figure 5 and the long section in Figure 6, the edge field strength is almost the same, namely about 1 Tesla, but the extension of the outside fringe fields behaves differently. The outside fringe fields of the short section vanish rapidly, but those of the long section cannot vanish even for a very long distance. By setting the inner radius of the solenoids to 1/10 of the original radius while keeping all the other parameters fixed, we computed the linear maps for the hard edge model and the correct fringe field treatment for finitely long solenoids, and we found reasonable agreement.

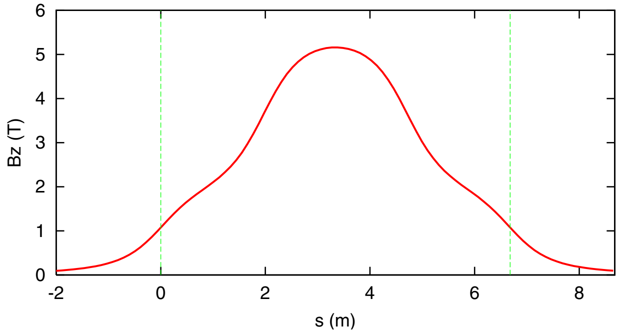


**Figure 6.** The axial magnetic field profile of the long section with finitely long solenoids and fringe fields.

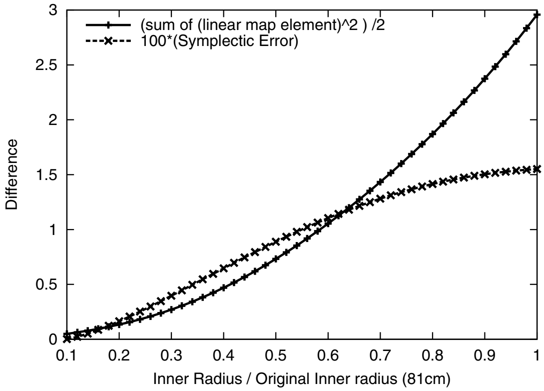


**Figure 7.** The disagreement of the linear transfer maps between the hard edge model and the correct fringe field treatment for the finitely long solenoids of the long section as functions of the aperture.

**Hard edge model with finitely long solenoids with linear kicks**
**(The inner radius is 1/10 of the original size.)**

```
-0.1162300E-01-0.1163328E-01 0.2318096      0.3343426      1000
 0.9834308E-01-0.4517004E-02 -2.826397      0.2320568      0100
```

**Finitely long solenoids with correct fringe field consideration**
**(The inner radius is 1/10 of the original size.)**

```
-0.5651780E-02-0.8030099E-02 0.2324166      0.3343818      1000
 0.6789750E-01-0.5511159E-02 -2.827323      0.2324200      0100
```

Figure 7 shows the correlation of the agreement of the maps for various aperture sizes. The difference in the sum of the square of linear terms and the difference in the symplectic error are plotted as functions of the ratio of the inner radius to the original size.

## 3. Dynamics through the magnets in the ring

Since one half of the ring characterizes the whole system as seen in Figure 1, we compute the transfer map of one half of the ring to study the beam dynamics through many revolutions in the ring. Scanning the energies of the reference particle shows that under the presence of dipole fringe fields and solenoid fringe fields, the linear motion is frequently unstable, suggesting the need to re-fit the optical properties of the ring. To illustrate the performance, we thus restricted ourselves to the design energy of 250 MeV total (=kinetic energy + muon mass energy). Figures 8 and 9 show tracking for various cases. Figure 8 shows the hard edge model of the solenoid with finitely long solenoids in the linear kick approximation. The left picture shows tracking at order 9 with a hard edge model bending magnet, while the right picture shows the effect of using a realistic bending magnet fringe field, which here leads to unstable linear motion. Figure 9 shows the finitely long solenoids with correct fringe field

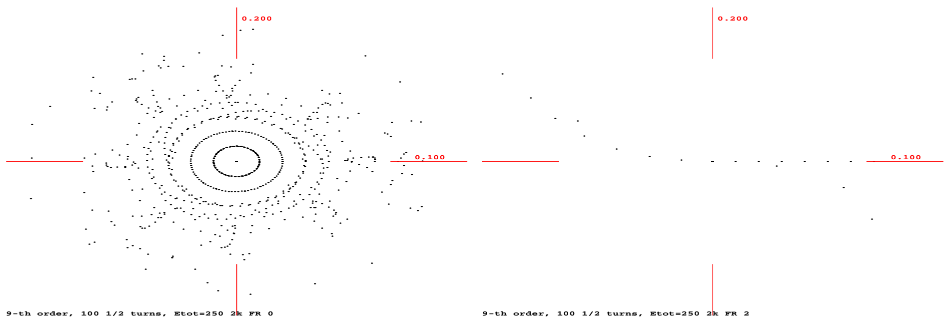


**Figure 8.** Tracking 50 revolutions at reference energy of $E_{tot}$ =250 MeV with finitely long solenoids in hard edge kick approximation, using hard edge dipole fields (left) and realistic dipole fringe fields (right).

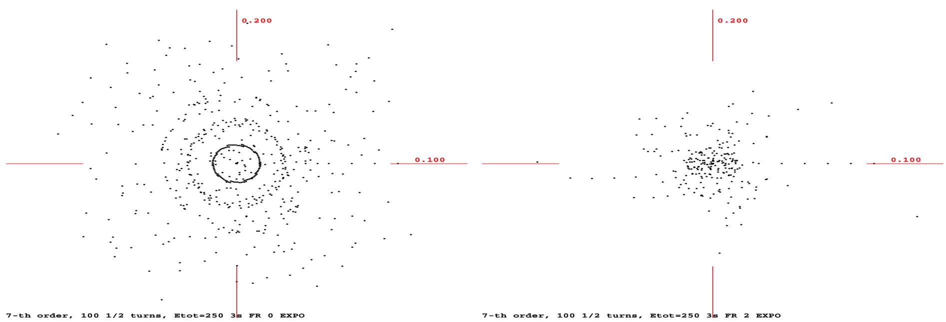


**Figure 9.** Tracking 50 revolutions at reference energy of $E_{tot}$ =250 MeV with finitely long solenoids with correct fringe field consideration, using hard edge dipole fields (left) and realistic dipole fringe fields (right).

consideration; again the left picture shows the situation for a hard-edge bending magnet, while the right picture shows the effects of a realistic bending magnet fringe field.

Particle tracking in the $x$-$a$ phase space is done for 50 full revolutions in the ring, and the Poincare sections are in the middle of the short straight solenoidal section, i.e. the upper left corner of Figure 1. In Figures 8 and 9, the horizontal axis is the horizontal position $x$ in meter, and the vertical axis is the horizontal slope $a = p_x/p_0$. The particles with the initial positions 1, 2, ..., 7 cm are tracked in the ring, and the ends of lines showing the axes in the pictures are $\pm 0.1$ meter in $x$ and $\pm 0.2$ in $a$.

## Acknowledgments

We are thankful to V. Balbekov for providing all the necessary details for the simulation as well as the pictures in Figures 1 through 4 to illustrate the system. The work was supported by the Illinois Consortium for Accelerator Research, the US Department of Energy, and the National Science Foundation.

## References

[1] V. Balbekov. Ring cooler progress. The Muon Collider and Neutrino Factory Notes MUC-NOTE-COOL-THEORY-0246, Fermi National Accelerator Laboratory, 2002. See http://www-mucool.fnal.gov/notes/notes.html.

[2] S. Ozaki et al. for the Muon Collaboration. Feasibility study-II of a muon-based neutrino source. Technical Report 52623, Muon Collider Collaboration, BNL, 2001.

[3] A. N. Skrinsky and V. V. Parkhoumchuk. Methods of cooling beams of charged particles. *Soviet Journal of Particles and Nuclei*, 12:223–247, 1981.

[4] D. Neuffer. Principles and applications of muon cooling. *Particle Accelerators*, 14:75–90, 1983.

[5] Ya. S. Derbenev. The self-cooling of charged particle beams in a straight line. Technical report, Department of Physics, University of Michigan, 1991.

[6] D. Errede, M Berz, C. J. Johnstone, K. Makino, and A. van Ginneken. Stochastic processes in muon ionization cooling. *Nuclear Instruments and Methods*, in print, 2003.

[7] K. Makino, M. Berz, D. Errede, and C. J. Johnstone. High order map treatment of superimposed cavities, absorbers, and magnetic multipole and solenoid fields. *Nuclear Instruments and Methods*, in print, 2003.

[8] K. Makino and M. Berz. Solenoid elements in COSY INFINITY. In these proceedings.

[9] M. Berz and K. Makino. COSY INFINITY Version 8.1 - user's guide and reference manual. Technical Report MSUHEP-20704, Department of Physics and Astronomy, Michigan State University, East Lansing, MI 48824, 2001. See also http://cosy.pa.msu.edu.

[10] V. Balbekov. Private communication, 2002.